Progress In Electromagnetics Research M, Vol. 37, 41–50, 2014

Magnitude Constraint Minimum Variance Beamformer with Conjugate Symmetric Constraint and Norm Constraint

Lulu Zhao[1, 2 *], Guang Liang[1, 2], and Huijie Liu[1, 2]

Abstract—In this paper, an improved robust minimum variance beamformer against direction of arrival (DOA) mismatch and finite sample effect is proposed. Multiple inequality magnitude constraints are imposed to broaden the main lobe of beampattern. The conjugate symmetric structure of the optimal weight is utilized to transform the non-convex inequality magnitude constraints into convex ones. A quadratic constraint on the norm of weight is introducing to make further improvement on robustness against DOA mismatch and finite sample effect. The proposed beamforming problem can be reformulated in the form of the second order cone programming and solved efficiently by interior point method. Simulation results show that the proposed beamformer outperforms several other adaptive beamformers.

1. INTRODUCTION

Adaptive arrays with data-dependent beamformers have been widely utilized in wireless communications, modern radar, sonar and medical imaging due to the anti-interference capability and superior resolution [1–3]. Standard Capon beamformer based on minimum variance distortionless response (MVDR) principle can provide maximum signal-to-interference-and-noise ratio (SINR) in the direction of arrival (DOA) of signal of interest (SOI) [4]. Therefore, it is the most popular one used in adaptive beamforming among the data-dependent beamformers. However, the performance of standard Capon beamformer is well known to be sensitive to DOA mismatch between the actual DOA of SOI and the presumed one [5]. If the presumed DOA deviates from the actual DOA of SOI, the standard Capon beamformer tends to suppress the SOI component. This effect is commonly referred to as signal self-nulling effect [6]. A similar effect occurs in the case that the error between ideal array covariance matrix and estimated array covariance matrix is too large when the number of snapshots used to estimate the array covariance matrix is small [7, 8]. Thus, many techniques called robust Capon beamformer (RCB) have been proposed to improve the robustness of the standard Capon beamformer against the DOA mismatch and estimation error of the array covariance matrix in the past decades ([9–16], and many references therein).

One popular and widely used method is the so-called diagonal loading technique, where the array covariance matrix is diagonally loaded with a scaled identity matrix [17]. However, the main drawback of this technique is that it is not clear how to choose the diagonal loading level based on information about the uncertainty of the DOA of SOI. An approach based on the optimization of the worst-case performance of the robust beamfomer (WCPRB) in the spherical uncertainty set of steering vector of SOI is developed in [18]. The doubly constrained robust Capon beamformer (DCRCB) which is introduced in [19] achieves robustness against DOA mismatch by enforcing a double constraint on the array steering vector, viz. a constant norm constraint and a spherical uncertainty set constraint on the steering vector of SOI. However, both the two methods require the error bound of steering vector

Received 28 April 2014, Accepted 9 May 2014, Scheduled 16 June 2014

* Corresponding author: Lulu Zhao (zhaolulu333nju@163.com).

[1] Shanghai Institute of Microsystem and Information Technology, Chinese Academy of Science, China. [2] Shanghai Engineering Center for Microsatellites, China.

which is hard to preset in some practical applications. The linear constraint minimum variance (LCMV) method uses equality linear constraints to force the responses near the DOA of SOI to be unity, which broadens the main lobe of the beampattern and improves the robustness of adaptive beamforming against DOA mismatch [20, 21]. However, the LCMV beamformer could not achieve the best SINR performance due to the deviation between the optimal array responses and the preset unity-ones in the constrained directions.

In this paper, we propose an improved robust minimum variance beamformer against DOA mismatch and finite sample effect. The equality linear constraints of LCMV beamformer are substituted by the inequality constraints on the magnitude response, which is more applicable to controlling the main lobe response of beampattern. However, the magnitude constraint with lower bound is non-convex, and the beamforming problem is not a convex optimization problem and cannot be solved by the well-established conventional convex optimization techniques directly. It can be proved that the optimum weight that maximizes output SINR is complex conjugate symmetric over the middle index for the commonly used centrosymmetric array structure, e.g., uniform linear array (ULA), hexagonal planar array (HPA) and so on [22]. By enforcing an additional conjugate symmetric constraint on the weight, the non-convex magnitude constraint can be transformed into a convex one without any relaxation or approximation when the array elements are symmetrically distributed. An additional norm constraint on the weight vector could make further improvement on the robustness against DOA mismatch and finite sample effect. A numerical method based on the quadratic program is provided to calculate the upper bound value of the norm constraint. It turns out that the original formulation of the proposed beamforming problem can be converted into second order cone programming (SOCP) form and solved efficiently in polynomial time via the well-established interior point method [23].

The remaining part of this paper is organized as follows. Both the standard Capon beamformer and LCMV beamformer are reviewed in Section 2. The improved robust minimum variance beamformer is proposed in Section 3. To verify the validity of the proposed robust beamformer, simulation results are presented and discussed in Section 4. The concluding remarks are given in Section 5.

2. SIGNAL MODEL AND PROBLEM FORMULATION

Suppose that there are $P+1$ narrowband signals impinging on the array with M elements. Let $\mathbf{x}(k)$ denote the kth sample vector of signal received by the array. The kth sample vector of received signal $\mathbf{x}(k)$ can be represented as

$$\mathbf{x}(k) = s_0(k)\mathbf{a}(\theta_0) + \sum_{j=1}^{P} i_j(k)\mathbf{a}(\theta_j) + \mathbf{n}(k) \tag{1}$$

where s_0, i_j and $\mathbf{n}$ are SOI, jth interference and noise, respectively. $\mathbf{a}(\theta)$ denotes the steering vector of DOA θ. The output of the beamformer $y(k)$ can be expressed as

$$y(k) = \mathbf{w}^H\mathbf{x}(k) \tag{2}$$

where $\mathbf{w}$ is the complex weight applied to the received signals at elements of array.

The SINR of an array output is one of the most popular quantities to evaluate the performance of adaptive beamforming. The variance of output signal in (2) is given by

$$E\left[|y(k)|^2\right] = \left|\mathbf{w}^H\mathbf{a}(\theta_0)\right|^2\sigma_0^2 + \sum_{j=1}^{P}\left|\mathbf{w}^H\mathbf{a}(\theta_j)\right|^2\sigma_j^2 + \mathbf{w}^H\mathbf{w}\sigma_n^2 = P_s + P_i + P_n \tag{3}$$

where $\mathbf{w}^H\mathbf{a}(\theta)$ is the array response in direction θ. σ_0^2, σ_j^2, σ_n^2 are the input powers of SOI, jth interference, and noise, respectively. Then, P_s, P_i, and P_n denote the output powers of SOI, interferences and noise, respectively. Accordingly, the output SINR of the beamformer is given by

$$\mathrm{SINR} = \frac{P_s}{P_i + P_n} = \frac{\left|\mathbf{w}^H\mathbf{a}(\theta_0)\right|^2\sigma_0^2}{\sum\limits_{i=1}^{P}|\mathbf{w}^H\mathbf{a}(\theta_i)|^2\sigma_i^2 + \mathbf{w}^H\mathbf{w}\sigma_n^2} = \frac{\left(\left|\mathbf{w}^H\mathbf{a}(\theta_0)\right|^2 \Big/ \mathbf{w}^H\mathbf{w}\right)(\sigma_0^2/\sigma_n^2)}{\sum\limits_{i=1}^{P}\left(\left|\mathbf{w}^H\mathbf{a}(\theta_\mathbf{i})\right|^2 \Big/ \mathbf{w}^H\mathbf{w}\right)(\sigma_i^2/\sigma_n^2) + 1} \tag{4}$$

where $|\mathbf{w}^H\mathbf{a}(\theta)|^2/\mathbf{w}^H\mathbf{w}$ is the white noise gain (WNG) in direction θ [24], σ_0^2/σ_n^2 the input signal-to-noise-ratio (SNR) of SOI, and σ_j^2/σ_n^2 the input interference-to-noise-ratio (INR) of jth interference.

The weight of standard Capon beamformer is chosen to minimize the output power of the beamformer while constraining the response in DOA of SOI to be unity. The standard Capon beamformer can be formulated as:

$$\min_{\mathbf{w}} \mathbf{w}^H\mathbf{R}_\mathbf{x}\mathbf{w} \quad \text{subject to } \mathbf{a}^H(\theta_0)\mathbf{w} = 1 \tag{5}$$

where $\mathbf{R}_\mathbf{x}$ is the data covariance matrix given by

$$\mathbf{R}_\mathbf{x} = E\{\mathbf{x}(k)\mathbf{x}^H(k)\} = \sigma_0^2\mathbf{a}(\theta_0)\mathbf{a}^H(\theta_0) + \sum_{j=1}^{P}\sigma_j^2\mathbf{a}(\theta_j)\mathbf{a}^H(\theta_j) + \sigma_n^2\mathbf{I} \tag{6}$$

where $\mathbf{I}$ is $M \times M$ identity matrix. The optimal weight of the standard Capon beamformer can be written as [4]

$$\mathbf{w}_C = \frac{\mathbf{R}_\mathbf{x}^{-1}\mathbf{a}(\theta_0)}{\mathbf{a}^H(\theta_0)\mathbf{R}_\mathbf{x}^{-1}\mathbf{a}(\theta_0)} \tag{7}$$

For an array whose elements are symmetrically distributed, the steering vector $\mathbf{a}(\theta)$ can be expressed in the form that is complex conjugate symmetric over the middle index as follow [13]

$$\mathbf{a}(\theta) = \mathbf{J}\mathbf{a}^*(\theta) \tag{8}$$

where $(\,)^*$ denotes the conjugate operation and $\mathbf{J}$ is the $M \times M$ exchange matrix defined as

$$\mathbf{J} = \begin{bmatrix} 0 & \dots & 0 & 1 \\ 0 & \dots & 1 & 0 \\ \vdots & \iddots & \vdots & \vdots \\ 1 & \dots & 0 & 0 \end{bmatrix} \tag{9}$$

Then, it can be proven that optimal weight follows generalized conjugate symmetric structure

$$\mathbf{w}_C = \mathbf{J}\mathbf{w}_C^* \tag{10}$$

Proof: let us define the real number $\mu = (\mathbf{a}^H(\theta_0)\mathbf{R}_\mathbf{x}^{-1}\mathbf{a}(\theta_0))^{-1}$, then $\mathbf{w}_C$ in (7) can be represented as

$$\mathbf{w}_C = \mu\mathbf{R}_\mathbf{x}^{-1}\mathbf{a}(\theta_0) \tag{11}$$

Since $\mathbf{R}_\mathbf{x}$ is the Hermitian Toeplitz matrix in (6), we have

$$\begin{aligned} \mathbf{J}\mathbf{R}_\mathbf{x}^*\mathbf{J} &= \mathbf{J}\left(\sigma_0^2\mathbf{a}^*(\theta_0)\mathbf{a}^T(\theta_0) + \sum_{j=1}^{P}\sigma_j^2\mathbf{a}^*(\theta_j)\,\mathbf{a}^T(\theta_j) + \sigma_n^2\mathbf{I}\right)\mathbf{J} \\ &= \sigma_0^2(\mathbf{J}\mathbf{a}^*(\theta_0))\left(\mathbf{a}^T(\theta_0)\mathbf{J}\right) + \sum_{j=1}^{P}\sigma_j^2\left(\mathbf{J}\mathbf{a}^*(\theta_j)\right)\left(\mathbf{a}^T(\theta_j)\mathbf{J}\right) + \sigma_n^2\mathbf{I} \\ &= \sigma_0^2\mathbf{a}(\theta_0)\mathbf{a}^H(\theta_0) + \sum_{j=1}^{P}\sigma_j^2\mathbf{a}(\theta_j)\,\mathbf{a}^H(\theta_j) + \sigma_n^2\mathbf{I} = \mathbf{R}_\mathbf{x} \end{aligned} \tag{12}$$

Note that $\mathbf{J}^{-1} = \mathbf{J}$, then

$$\begin{aligned} \mathbf{J}\mathbf{w}_C^* &= \mu\mathbf{J}(\mathbf{R}_\mathbf{x}^{-1}\mathbf{a}(\theta_0))^* = \mu\mathbf{J}^{-1}\left(\mathbf{R}_\mathbf{x}^{-1}\right)^*\mathbf{J}^{-1}\mathbf{J}\mathbf{a}^*(\theta_0) \\ &= \mu(\mathbf{J}\mathbf{R}_\mathbf{x}^*\mathbf{J})^{-1}\mathbf{a}(\theta_0) = \mu\mathbf{R}_\mathbf{x}^{-1}\mathbf{a}(\theta_0) = \mathbf{w}_C \end{aligned} \tag{13}$$

The result in (10) can be obtained.

In practical applications, since the actual DOA of SOI θ_0 is not always precisely known, a presumed one $\widehat{\theta}_0$ is often applied in standard Capon beamformer. On the other hand, the ideal data covariance matrix $\mathbf{R}_\mathbf{x}$ is usually estimated by the finite sample vector of received signal as follow

$$\widehat{\mathbf{R}}_\mathbf{x} = \frac{1}{K}\sum_{k=1}^{K}\mathbf{x}^H(k)\mathbf{x}(k) \tag{14}$$

K is the number of snapshots. Using the presumed DOA of SOI $\widehat{\theta}_0$ and estimated data covariance matrix $\widehat{\mathbf{R}}_{\mathbf{x}}$, the weight in (7) can be rewritten as

$$\widehat{\mathbf{w}}_C = \frac{\widehat{\mathbf{R}}_{\mathbf{x}}^{-1}\mathbf{a}(\widehat{\theta}_0)}{\mathbf{a}^H(\widehat{\theta}_0)\widehat{\mathbf{R}}_{\mathbf{x}}^{-1}\mathbf{a}(\widehat{\theta}_0)} \tag{15}$$

When the presumed DOA $\widehat{\theta}_0$ is different from the actual DOA of SOI θ_0, the standard Capon beamformer may mistake the SOI for interference and tend to suppress SOI. This effect is commonly referred to as signal self-nulling. The performance of standard Capon beamformer also can be degraded by the data covariance matrix error between the ideal one and estimated one, especially K is small.

The LCMV beamformer could improve the robustness against DOA mismatch through imposing a set of linear unity-response constraints around the presumed DOA of SOI. The LCMV beamforming problem can be expressed as

$$\min_{\mathbf{w}} \mathbf{w}^H\mathbf{R}_{\mathbf{x}}\mathbf{w} \text{ subject to } \mathbf{C}^H\mathbf{w} = \mathbf{f} \tag{16}$$

where $\mathbf{C}$ is the $M \times l$ matrix containing l steering vectors in the constrained directions. $\mathbf{f} = [1, 1, \ldots 1]^T$ is the $l \times 1$ response vector. The optimal weight vector solution for the LCMV beamformer is given by [21]:

$$\mathbf{w}_L = \mathbf{R}_{\mathbf{x}}^{-1}\mathbf{C}\left(\mathbf{C}^H\mathbf{R}_{\mathbf{x}}^{-1}\mathbf{C}\right)^{-1}\mathbf{f} \tag{17}$$

The array responses around the presumed DOA of SOI are set to be unity. However, since array responses in the constrained directions of the optimal weight $\mathbf{w}_C$ are usually unequal, the unity-response constraints are not always the optimal constraints, which are hard to preset in practical application. The performance of LCMV beamformer could be degraded by the deviation between the optimal array responses and the preset unity-response in the constrained directions.

3. THE IMPROVED ROBUST MINIMUM VARIANCE BEAMFORMER

3.1. The Proposed Robust Beamformer

A reasonable method to improve the performance of LCMV beamformer is that only the magnitude responses in constrained directions are set to exceed unity while the output variance is minimized. The inequality magnitude constraint minimum variance beamformer can be represented as

$$\min_{\mathbf{w}} \mathbf{w}^H\mathbf{R}_{\mathbf{x}}\mathbf{w} \quad \text{subject to } \left|\mathbf{w}^H\mathbf{a}(\varphi_i)\right| \geq 1, \quad i = 1, 2, \ldots, l \tag{18}$$

It can be seen that (18) is not a convex optimization problem due to the presence of the non-convex constraints $|\mathbf{w}^H\mathbf{a}(\varphi_i)| \geq 1$, $i = 1, 2, \ldots, l$. As a result, the well-established conventional convex programming techniques are not directly applicable. Since it is shown in Section 2 that the optimal weight is conjugate symmetric for the commonly used centrosymmetric array structure, the conjugate symmetric constraint on the weight is introduced to the proposed robust beamformer. Then, the inequality magnitude constraint minimum variance beamformer with conjugate symmetric constraint can be formulated as follows:

$$\begin{gathered}\min_{\mathbf{w}} \mathbf{w}^H\mathbf{R}_{\mathbf{x}}\mathbf{w} \quad \text{subject to } \left|\mathbf{w}^H\mathbf{a}(\varphi_i)\right| \geq 1, \quad i = 1, 2, \ldots, l, \\ \mathbf{w} = \mathbf{J}\mathbf{w}^*\end{gathered} \tag{19}$$

Considering both $\mathbf{w}$ and $\mathbf{a}(\varphi_i)$ are conjugate symmetric, we have

$$\mathbf{w}^H\mathbf{a}(\varphi_i)=(\mathbf{J}\mathbf{w}^*)^H(\mathbf{J}\mathbf{a}^*(\varphi_i))=(\mathbf{w}^H)^*\mathbf{J}^H\mathbf{J}\mathbf{a}^*(\varphi_i) = (\mathbf{w}^H\mathbf{a}(\varphi_i))^* \tag{20}$$

It is proven that the array response $\mathbf{w}^H\mathbf{a}(\theta_i)$ is real number. Without loss of generality, supposing all the array response around the DOA of SOI to be positive, problem in (19) can be rewritten as:

$$\begin{gathered}\min_{\mathbf{w}} \mathbf{w}^H\mathbf{R}_{\mathbf{x}}\mathbf{w} \quad \text{subject to } \mathbf{w}^H\mathbf{a}(\varphi_i) \geq 1, \quad i = 1, 2, \ldots, l \\ \mathbf{w} = \mathbf{J}\mathbf{w}^*\end{gathered} \tag{21}$$

To make further improvement on the robustness against DOA mismatch and finite sample effect, an additional quadratic inequality constraint on the Euclidean norm of the weight vector is imposed [25]. This requires incorporating the quadratic inequality constraint on $\mathbf{w}$ of the form:

$$\mathbf{w}^H\mathbf{w} \leq \eta \tag{22}$$

The inequality magnitude constraint minimum variance beamformer with conjugate symmetric constraint and norm constraint can be represented as follows:

$$\begin{aligned} \min_{\mathbf{w}} \mathbf{w}^H\mathbf{R}_{\mathbf{x}}\mathbf{w} \quad \text{subject to } & \mathbf{w}^H\mathbf{a}(\varphi_i) \geq 1, \quad i = 1, 2, \ldots, l \\ & \mathbf{w} = \mathbf{J}\mathbf{w}^* \\ & \mathbf{w}^H\mathbf{w} \leq \eta \end{aligned} \tag{23}$$

Let $\mathbf{R}_{\mathbf{x}} = \mathbf{Q}^H\mathbf{Q}$, where $\mathbf{Q}$ is the Cholesky factorization. Then, the objective function of (23) becomes:

$$\mathbf{w}^H\mathbf{R}_{\mathbf{x}}\mathbf{w} = \mathbf{w}^H\mathbf{Q}^H\mathbf{Q}\mathbf{w} = |\mathbf{Q}\mathbf{w}|^2 \tag{24}$$

Introducing $|\mathbf{Q}\mathbf{w}| \leq \tau$, the optimization problem in (23) can be converted into the following SOCP problem [26]

$$\begin{aligned} \min_{\tau,\mathbf{w}} \tau \quad \text{subject to } & |\mathbf{Q}\mathbf{w}| \leq \tau \\ & \mathbf{w}^H\mathbf{a}(\varphi_i) \geq 1, \quad i = 1, 2, \ldots, l \\ & \mathbf{w} = \mathbf{J}\mathbf{w}^* \\ & |\mathbf{w}| \leq \sqrt{\eta} \end{aligned} \tag{25}$$

The SOCP problem (25) can be easily solved using standard and highly efficient interior point method software tool, such as SeDuMi convex optimization Matlab toolbox [27].

3.2. Setting the Norm Constraint

Consider the value of the parameter in the norm constraint which plays an important role to the performance of the proposed RBF. In order to draw the lower bound of η, we consider the problem as follow:

$$\begin{aligned} \min_{\mathbf{w}} \mathbf{w}^H\mathbf{w} \quad \text{subject to } & \mathbf{w}^H\mathbf{a}(\varphi_i) \geq 1, i = 1, 2, \ldots, l \\ & \mathbf{w} = \mathbf{J}\mathbf{w}^* \end{aligned} \tag{26}$$

The convex optimization problem (26) is a quadratic program (QP), which can be solved by the well-known active set method [28].

Assume that the minimum value of problem (26) is $\eta_{\min}$. Let $\mathbf{S}$ be the set defined by the constraints in the optimization problem (23), namely

$$\mathbf{S} = \left\{\mathbf{w} | \mathbf{w}^H\mathbf{a}(\varphi_i) \geq 1, \quad i = 1, 2, \ldots, l, \quad \mathbf{w} = \mathbf{J}\mathbf{w}^*, \quad \mathbf{w}^H\mathbf{w} \leq \eta\right\} \tag{27}$$

When the parameter $\eta < \eta_{\min}$, the set $\mathbf{S}$ is an empty set. In other words, $\eta_{\min}$ is the lowest allowable value for η to keep the set $\mathbf{S}$ nonempty. However, if η is set to be the lowest allowable value $\eta_{\min}$, it can be seen from (3) and (26) that the $\mathbf{w}$ only minimizes the output noise power P_n without considering the suppression of interference. On the other hand, if the parameter η approaches infinity, the norm constraint will fail to improve the robustness of the proposed robust beamformer. The choice of the norm constraint value reflects a design tradeoff between interference suppression and robustness over system mismatch. So, in the interference presented environment, the norm constraint could be relaxed as follow

$$\mathbf{w}^H\mathbf{w} \leq \eta_{\min} + \delta \tag{28}$$

where $\delta > 0$ is a positive number. A reasonable norm constraint value is $\delta = 0.05\eta_{\min}$ or, equivalently $\eta = 1.05\eta_{\min}$.

4. SIMULATION RESULTS

In this section, simulations of the proposed robust beamformer (RBF) are carried out, and the results are compared with other beamformers, i.e., standard Capon beamformer, LCMV beamformer, robust beamformer using worst-case performance optimization (WCPRB), doubly constrained robust Capon beamformer (DCRCB). Without loss of generality, we assume a ULA with $M = 10$ elements and half-wavelength spacing between adjacent elements (i.e., $d = \lambda/2$). There are three signals impinging upon the array, the SOI s_0 with actual DOA θ_0 and two uncorrelated interferences i_1 and i_2 with DOAs $\theta_1 = 30°$ and $\theta_2 = 70°$, respectively. The INRs of i_1 and i_2 are 40 dB and 20 dB, respectively. All results are averaged over 100 independent simulations.

4.1. SINR versus SNR

In this example, the actual DOA of SOI $\theta_0 = 43°$ while the presumed DOA $\widehat{\theta}_0 = 45°$. Three constraints on $\varphi_1 = 42°$, $\varphi_2 = 45°$ and $\varphi_3 = 48°$ are applied in both the proposed RBF and LCMV beamformer. The minimum norm of weight $\eta_{\min}$ optimized by (26) is 0.112, and the parameter of the norm constraint η is set to 0.118 according to (28). The parameter ϵ of the spherical uncertainty set in DCRCB is set as recommended in [19]

$$\epsilon \geq \max_{\varphi_1 \leq \varphi \leq \varphi_3} \left\{ \min_{\alpha} \left\| \mathbf{a}(\varphi) e^{j\alpha} - \mathbf{a}(\varphi_2) \right\| \right\} \approx 1 \tag{29}$$

The parameter ε in WCPRB [18] equals the square root of ϵ, then ε is set to be 1. The output SINRs are compared for different input SNRs ranging from -15 dB to 25 dB. No finite-sample effect is considered and all results have been computed using the exact array covariance matrix $\mathbf{R_x}$.

The SINR of standard Capon beamformer without DOA mismatch in the ideal case is also plotted as an upper bound of performance. The results are shown in Fig. 1. The SINR of the standard Capon beamformer is seriously degraded with 2° DOA mismatch compared with the ideal case, especially in high SNR region. When the SNR increases, the standard Capon beamformer tends to suppress the strong SOI to minimize the total output variance of beamformer. The LCMV beamformer has good performance in the high SNR region compared to standard Capon beamformer, but also inferior to other robust beamformers. In this example, the SINR performance of proposed RBF is very close to the upper bound in the ideal case without DOA mismatch. It is obviously demonstrated that the proposed RBF has better SINR performance than DCRCB and WCPRB as the input SNR increases higher than 10 dB.

The WNG beampatterns of all mentioned beamformers for SNR = 10 dB are shown in Fig. 2. The WNGs in the DOAs θ_0, θ_1 and θ_2 of beampatterns in Fig. 2 and output SINRs for input SNR = 10 dB are listed in Table 1. The vertical solid line in Fig. 2 shows the DOA of SOI and the vertical dash lines show the DOAs of two interferers. It can be seen that the standard Capon beamformer forms null near the DOA of SOI because of the self-nulling effect and the WNG in the DOA θ_0 is only -14 dB, which shows

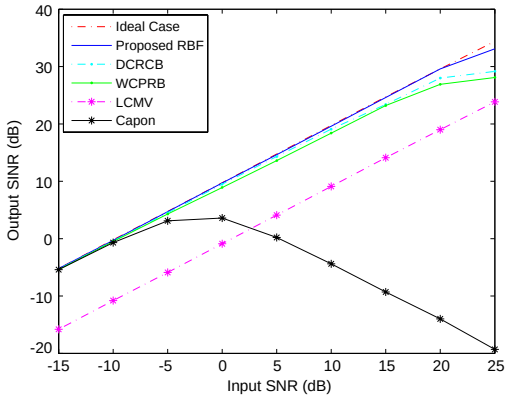

Figure 1. Output SINR versus input SNR.

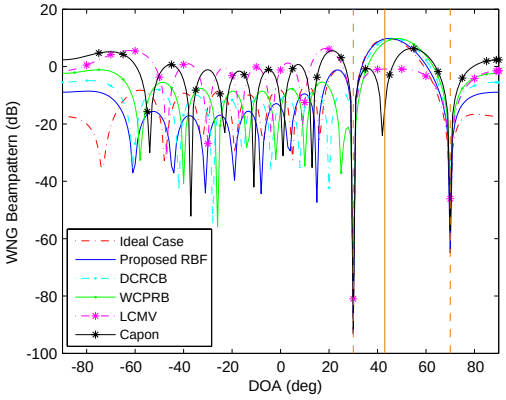

Figure 2. WNG Beampattern (SNR = 10 dB).

Table 1. The WNGs in the DOA of SOI and interferences and output SINRs (SNR = 10 dB).

	WNG			SINR
	θ_0 (dB)	θ_1 (dB)	θ_2 (dB)	(dB)
Ideal Case	9.75	−92	−53	19.74
Proposed RBF	9.6	−88	−65	19.6
DCRCB	9.3	−70	−35	19.1
WPRCB	8.5	−74	−44	18.4
LCMV	−0.8	−80	−46	9.1
Capon	−14	−93	−57	−4.4

the poor noise suppression ability of standard Capon beamformer when DOA mismatch is presented. The LCMV beamformer forms flat beam around the DOA of SOI to improve robustness against DOA mismatch. However, it also fails to form the mainlobe around the actual DOA of SOI. The WNGs in DOA θ_0 of LCMV beamformer is −0.8 dB, which results in 10.5 dB SINR performance loss compared with the proposed RBF. The output SINR of the proposed RBF achieves a better performance with 0.5 dB and 1.2 dB higher than DCRCB and WCPRB, respectively, yet only 0.14 dB lower than the ideal case. This is because the proposed RBF forms a main lobe closest to the ideal case and the deepest nullings in the DOAs of interferences among the robust beamformers.

4.2. SINR versus DOA Mismatch

In this example, the presumed DOA $\widehat{\theta}_0 = 45°$, and actual DOA θ_0 ranges from 41° to 49°. Three constraints on $\varphi_1 = 41°$, $\varphi_2 = 45°$ and $\varphi_3 = 49°$ are applied in both the proposed RBF and LCMV beamformer. The minimum norm of weight $\eta_{\min}$ optimized by (26) is 0.121 and the parameter of the norm constraint is set to be 0.127 according (28). the parameter ϵ of the spherical uncertainty set in DCRCB is set as follow

$$\epsilon \geq \max_{\varphi_1 \leq \varphi \leq \varphi_3} \left\{ \min_{\alpha} \left\| a(\varphi) e^{j\alpha} - a(\varphi_2) \right\| \right\} \approx 2 \tag{30}$$

then ε in WCPRB is set to $\sqrt{2}$. The output SINRs are compared for DOA mismatches ranging from −4° to 4°. No finite-sample effect is considered and all results have been computed using the exact array covariance matrix

$\mathbf{R_x}$.

The SINR of standard Capon beamformer without mismatch is also shown as an ideal case in the

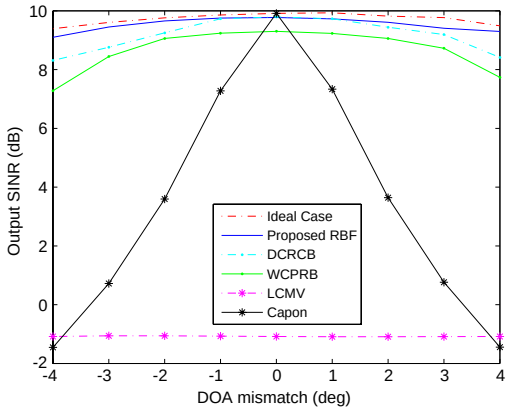

Figure 3. Output SINR versus DOA mismatch (SNR = 0 dB).

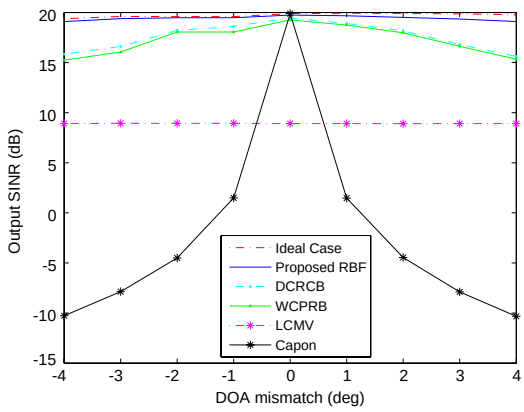

Figure 4. Output SINR versus DOA mismatch (SNR = 10 dB).

following figures. The results for SNR = 0 dB are displayed in Fig. 3 and the results for SNR = 10 dB are displayed in Fig. 4. It can be observed that the standard Capon beamformer is very sensitive to DOA mismatch. The standard Capon beamformer becomes more sensitive to DOA mismatch when the SNR is higher. The SINR decreases 30 dB as DOA mismatch range from 0° to 4° when the SNR is 10 dB. As a comparison, the SINR only decrease 12 dB when the SNR is 0 dB. The performance of LCMV beamformer is inferior to other robust beamformer apparently. In this example, the proposed RBF has the best SINR performance among robust beamformers and the output SINR of proposed RBF decreases slightly compared to the ideal case. The proposed RBF maintains steady SINRs whereas the SINRs of DCRCB and WCPRB decrease more than 3 dB with DOA mismatch varying from 0° to 4° when the input SNR is 10 dB.

4.3. SINR versus Number of Snapshots

The covariance matrices $\mathbf{R_x}$ used in the previous examples are assumed to be perfect without considering the finite-sample effect. In practice, the accuracy of the estimated covariance matrix $\widehat{\mathbf{R}}_\mathbf{x}$ affects the performance of the beamformers. The finite sample effect is considered in this example. Both perfect covariance matrix $\mathbf{R_x}$ and actual steering vector of SOI $\mathbf{a}(\theta_0)$ are applied in the ideal case. The impact of the finite sample effect on standard Capon beamformer is shown by using the estimated covariance matrix $\widehat{\mathbf{R}}_\mathbf{x}$ and considering no DOA mismatch. The parameters setting of other beamformers are the same with Subsection 4.1 and the results for SNR = 10 dB are shown in Fig. 5. It is shown that the standard Capon beamformer suffers from the finite-sample effect. The SINR decreases seriously when the number of the number of snapshots is less than 200. The other beamformers are effective against the finite-sample effect when the number of snapshots is over 100. The proposed RBF outperforms other robust beamformers and approaches the ideal case when the DOA mismatch is presented. This shows that the proposed RBF is robust against both the finite-sample effect and the DOA mismatch.

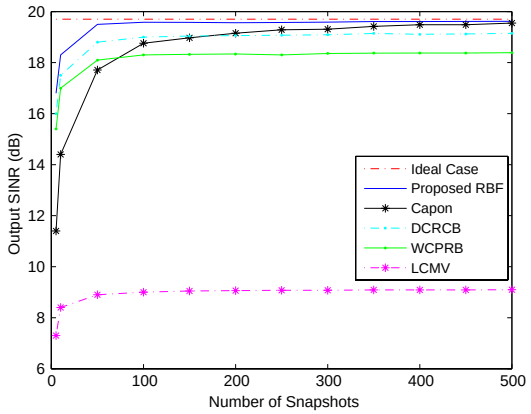

Figure 5. Output SINR versus number of snapshots.

4.4. Norm Constraint Parameter Selection Analysis

In this subsection, the relationship between the performance of proposed RBF and the norm constraint level η is discussed. The other parameters setting of proposed RBF are the same with Subsection 4.1.

The output SINR for input SNR = 10 dB and WNG in DOA of two interferences θ_1 and θ_2 versus norm constraint level η varying from $\eta_{\min}$ to $2\eta_{\min}$ are shown in Fig. 6. Let $\mathbf{w}_\eta$ denote the optimal weight of proposed RBF with given norm constraint level η. The norm square of $\mathbf{w}_\eta$ is denoted by K_η, i.e., $K_\eta = \mathbf{w}_\eta^H \mathbf{w}_\eta$. K_η and WNG in DOA of SOI θ_0 versus η are displayed in Fig. 7. We can see that if η approaches the lower bound $\eta_{\min}$, the WNGs in θ_1 and θ_2 are high, hence the two interferences are not suppressed sufficiently and the output SINR is very low. On the contrary, if η approaches $2\eta_{\min}$, the output SINR performance is degraded by the lowest WNG in θ_0. Meanwhile, K_η is unequal to the given norm constraint level η when η is large, which means that the norm constraint is inactive and

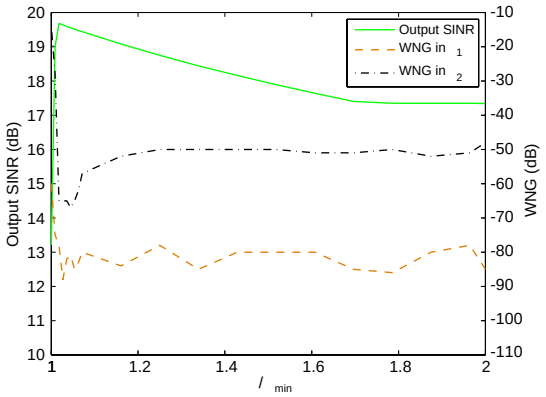

Figure 6. Output SINR and WNG in θ_1 and θ_2 versus norm constraint level (SNR = 10 dB).

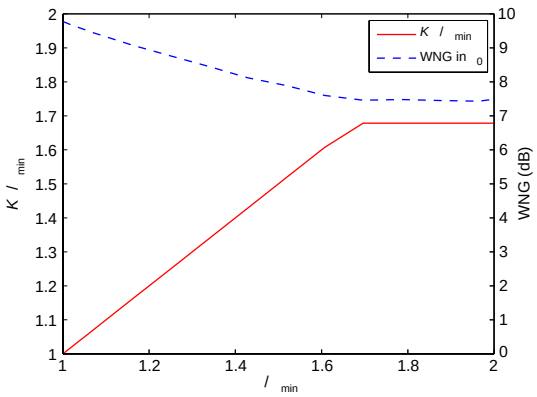

Figure 7. Norm square of optimal weight and WNG in θ_0 versus norm constraint level.

unable to improve the robustness of proposed RBF. The simulation results demonstrate that a proper norm constraint level (e.g., $\eta = 1.05\eta_{\min}$) should be selected to make improvement on robustness and SINR performance of proposed RBF.

5. CONCLUSIONS

In summary, a robust minimum variance beamformer against DOA mismatch and finite sample effect is proposed for symmetrically distributed arrays in this paper. The magnitude responses at the constrained directions are set to exceed unity, and these non-convex constraints with lower bound are converted into convex ones by introducing a conjugate symmetric constraint. A norm constraint on weight is imposed to make further improvement on the robustness against DOA mismatch and finite sample effect. The proposed RBF can be optimized by standard interior point method efficiently. The parameter of norm constraint is selected reasonably by quadratic program. The simulation results demonstrate the excellent performance of the proposed method.

ACKNOWLEDGMENT

This work was supported by the Innovation Foundation of Chinese Academy of Sciences (grant CXJJ-11-S107) and Natural Science Foundation of Shanghai (grant 11ZR1435000).

REFERENCES

1. Van Veen, B. D. and K. M. Buckley, "Beamforming: A versatile approach to spatial filtering," *IEEE Acoust., Speech, Signal Process. Mag.*, Vol. 5, No. 2, 4–24, 1988.
2. Godara, L. C., "Application of antenna arrays to mobile communications, Part II: Beam-forming and direction-of-arrival considerations," *Proc. IEEE*, Vol. 85, No. 8, 1195–1245, 1997.
3. Qu, Y., G. S. Liao, S. Q. Zhu, and X. Y. Liu, "Pattern synthesis of planar antenna array via convex optimization for airborne forward looking radar," *Progress In Electromagnetics Research*, Vol. 84, 1–10, 2008.
4. Capon, J., "High-resolution frequency-wavenumber spectrum analysis," *Proc. IEEE*, Vol. 57, No. 8, 1408–1418, 1969.
5. Wax, M. and Y. Anu, "Performance analysis of the minimum variance beamformer in the presence of steering vectors errors," *IEEE Trans. Signal Process.*, Vol. 44, No. 4, 938–947, 1996.
6. Van Trees, H. L., *Detection, Estimation and Modulation Theory, Part IV: Optimum Array Processing*, Wiley, New York, 2002.

7. Carlson, B. D., "Covariance matrix estimation errors and diagonal loading in adaptive arrays," *IEEE Trans. Aerosp. Electron. Syst.*, Vol. 24, No. 4, 397–401, 1988.
8. Wax, M. and Y. Anu, "Performance analysis of the minimum variance beamformer," *IEEE Trans. Signal Process.*, Vol. 44, No. 4, 928–937, 1996.
9. Stoica, P., Z. Wang, and J. Li, "Robust Capon beamforming," *IEEE Signal Process. Lett.*, Vol. 10, No. 6, 172–175, 2003.
10. Lorenz, R. G. and S. P. Boyd, "Robust minimum variance beamforming," *IEEE Trans. Signal Process.*, Vol. 53, No. 5, 1684–1696, 2005.
11. Lie, J. P., W. Ser, and C. M. S. See, "Adaptive uncertainty based iterative robust Capon beamformer using steering vector mismatch estimation," *IEEE Trans. Signal Process.*, Vol. 59, No. 9, 4483–4488, 2011.
12. Nai, S. E., W. Ser, Z. L. Yu, and H. Chen, "Iterative robust minimum variance beamforming," *IEEE Trans. Signal Process.*, Vol. 59, No. 4, 1601–1611, 2011.
13. Zaharis, Z. D., C. Skeberis, and T. D. Xenos, "Improved antenna array adaptive beamforming with low side lobe level using a novel adaptive invasive weed optimization method," *Progress In Electromagnetics Research*, Vol. 124, 137–150, 2012.
14. Liu, C. F. and J. Yang, "Robust LCMP beamformer with negative loading," *Progress In Electromagnetics Research*, Vol. 130, 541–561, 2012.
15. Chen, Y. L. and J. H. Lee, "Finite data performance analysis of MVDR antenna array beamformers with diagonal loading," *Progress In Electromagnetics Research*, Vol. 134, 475–507, 2013.
16. Yang, K., Z. Q. Zhao, and Q. H. Liu, "Robust adaptive beamforming against array calibration errors," *Progress In Electromagnetics Research*, Vol. 140, 341–351, 2013.
17. Li, J., P. Stoica, and Z. Wang, "On robust Capon beamforming and diagonal loading," *IEEE Trans. Signal Process.*, Vol. 51, No. 7, 1702–1715, 2003.
18. Vorobyov, S. A., A. B. Gershman, and Z. Q. Luo, "Robust adaptive beamforming using worst-case performance optimization: A solution to the signal mismatch problem," *IEEE Trans. Signal Process.*, Vol. 51, No. 2, 313–324, 2003.
19. Li, J., P. Stoica, and Z. Wang, "Doubly constrained robust Capon beamformer," *IEEE Trans. Signal Process.*, Vol. 52, No. 7, 2407–2423, 2004.
20. Booker, A. and C. Y. Ong, "Multiple constraint adaptive filtering," *Geophysics*, Vol. 36, No. 3, 498–509, 1971.
21. Frost, III, O. L., "An algorithm for linearly constrained adaptive array processing," *Proc. IEEE*, Vol. 60, No. 8, 926–935, 1972.
22. Huarng, K. C. and C. C. Yeh, "Adaptive beamforming with conjugate symmetric weights," *IEEE Trans. Signal Process.*, Vol. 39, No. 7, 926–932, 1991.
23. Boyd, S. and L. Vandenberghe, *Convex Optimization*, Cambrideg University Press, Cambridge, UK, 2004.
24. Cox, H., R. M. Zeskind, and M. M. Owen, "Robust adaptive beamforming," *IEEE Trans. Acoust., Speech, Signal Process.*, Vol. 35, No. 10, 1365–1376, 1987.
25. Tian, Z., K. L. Bell, and H. L. Van Trees, "A recursive least squares implementation for LCMP beamforming under quadratic constraint," *IEEE Trans. Signal Process.*, Vol. 49, No. 6, 1138–1145, 2001.
26. Liu, J., A. B. Gershman, Z. Q. Luo, and K. M. Wong, "Adaptive beamforming with sidelobe control: A second-order cone programming approach," *IEEE Signal Process. Lett.*, Vol. 10, No. 11, 331–334, 2003.
27. Strum, J. F., "Using SeDuMi 1.02, a Matlab toolbox for optimization over symmetric cones," *Optimization Methods and Software*, Vol. 11, Nos. 1–4, 625–653, 1999.
28. Luenberger, D. G. and Y. Y. Ye, *Linear and Nonlinear Programming*, Springer, New York, 2008.